Published in final edited form as:
Anal Chem. 2011 July 1; 83(13): 5107–5113. doi:10.1021/ac103271w.

IR and UV Photodissociation as Analytical Tools for Characterizing Lipid A Structures

James A. Madsen[1], **Thomas W. Cullen**[2], **M. Stephen Trent**[2,3], and **Jennifer S. Brodbelt**[1]

Jennifer S. Brodbelt: jbrodbelt@mail.utexas.edu

[1]Department of Chemistry and Biochemistry, The University of Texas at Austin, 1 University Station A5300, Austin, TX, USA 78712

[2]Section of Molecular Genetics and Microbiology, The University of Texas at Austin, Austin, TX, USA 78712

[3]The Institute of Cellular and Molecular Biology, The University of Texas at Austin, Austin, TX, USA 78712

Abstract

The utility of 193 nm ultraviolet photodissociation (UVPD) and 10.6 μm infrared multiphoton dissociation (IRMPD) for characterization of lipid A structures was assessed in an ion trap mass spectrometer. The fragmentation behavior of lipid A species was also evaluated by activated – electron photodetachment (a-EPD), which uses 193 nm photons to create charge reduced radicals that are subsequently dissociated by collisional activation. In contrast to collision induced dissociation (CID), IRMPD offered the ability to selectively differentiate product ions with varying degrees of phosphorylation due to the increased photoabsorption cross-sections and thus dissociation of phosphate-containing species. Both 193 nm UVPD and a-EPD yielded higher abundances and a larger array of product ions arising from C-C cleavages as well as cross-ring and inter-ring glucosamine cleavages compared to CID and IRMPD due to high energy, single photon absorption and/or radical-directed dissociation. UVPD at 193 nm also exhibited enhanced cleavage between the amine and carbonyl groups on the 2- and 2'-linked primary acyl chains. Lastly, UVPD of phosphorylethanolamine-modified lipid A species resulted in preferential cleavage of the C-O bond between ethanolamine and phosphate enabling the selective identification of this modification.

INTRODUCTION

Lipopolysaccharides (LPS), consisting of polysaccharide chains and a lipid core (lipid A), decorate the surfaces of Gram-negative bacteria. Lipid A, the anchor point for lipopolysaccharides to the cell membrane, is comprised of a diglucosamine backbone with various fatty acid appendages. During Gram-negative infections, dissociated LPS interacts with a variety of cell- and serum-binding proteins, leading to the activation of the innate immune system. Notably, it is the lipid A anchor that is the bioactive component of LPS.[1, 2]

Despite the conservation of the lipid A biosynthetic pathway, a large degree of heterogeneity is seen between the lipid A species generated by Gram-negative bacteria. This diversity arises in part from the action of enzymes that modify the lipid A structure following the conserved pathway. It has been proposed that pathogenic bacteria modulate their lipid A structure to avoid detection by the innate immune system. Changes in the acylation and/or

Correspondence to: Jennifer S. Brodbelt, jbrodbelt@mail.utexas.edu.

phosphorylation pattern of lipid A have a profound impact on the endotoxic nature of LPS.[1, 2] Modification of the lipid A structure also provides protection from cationic antimicrobial peptides (CAMPs) which are responsible for killing a variety of invading microbes. These peptides are initially attracted to the negative charges present on the Gram-negative outer membrane, including the phosphate groups of lipid A. Decoration of the phosphate groups with amine-containing substituents such as phosphorylethanolamine or L-4-aminoarabinose aids in CAMP resistance.[1, 2] Given the diversity seen in lipid A structures and the fact that the biological activity of lipid A largely arises from its substituent pattern, the structural characterization of lipid A species is a crucial and challenging task for any investigation of LPS.

Mass spectrometry has become an indispensable tool for the characterization of lipid A structures.[3] In particular, the employment of low-energy collision induced dissociation (CID) has yielded the identification and characterization of various lipid A structures from a number of bacterial species.[4-15] However, there remain several shortcomings of CID that limit its usefulness in molecular characterization of lipid A species. CID typically results in cleavage of the most labile bonds, thus resulting in fragmentation patterns that are often insufficient for mapping all functionalities and their positions in complex lipid A structures. This drawback also limits the ability to detect subtle (yet biologically important) modifications along the fatty acid chains. Furthermore, inter- and intra- ring cleavages of the glucosamine groups (i.e., resulting in “B”, “Y”, “C”, “Z” and “A”, “X” ions, respectively) are uncommon or occur in low abundance especially for the first MS^n stages.[9, 11-13, 15] These important diagnostic products facilitate mapping of the attachment sites of fatty acids, phosphorylations, phosphoethanolamines, and other substituents to the saccharide groups. Therefore, several stages of MS (i.e., MS^n) have been employed to increase the number and diversity of product ions for successful lipid A structural assignments,[6, 9, 11, 14-16] albeit with diminishing sensitivity at each step and depending on access to ample quantities of the lipids. High-energy (keV) CID on sector instruments has also been used previously to increase and diversify fragment ion productions (generally with liquid secondary ion mass spectrometry (liquid-SIMS) or fast atom bombardment (FAB) generation of ions),[17-19] methods that have been largely replaced by newer ESI and MALDI methods and lower energy CID. The framework for elucidation of oligosaccharides was developed over twenty years ago in which the initial applications and mechanisms of inter- and cross-ring cleavages by a variety of desorption ionization and tandem mass spectrometric methods were established.[20-27] The resulting ability to assign sequence and linkage information proved to be key for determination of the diglucosamine skeleton of lipid A structures. For example, an infrared laser desorption method promoted retro-aldol fragmentation reactions within the sugar rings of lipid A molecules, ultimately allowing elucidation of the positions of the fatty acyl groups.[20] Given the intricacies of lipid A characterization, the development and application of new and/or improved tandem mass spectrometric methods that can provide more comprehensive and predictable structural information are warranted.

As described in this report, three photodissociation methods, including infrared multiphoton dissociation (IRMPD), ultraviolet photodissociation (UVPD), and activated – electron photodetachment dissociation (a-EPD), are applied for the characterization of lipid A structures. IRMPD is an alternative MS/MS technique that utilizes multiple 10.6 μm photons for ion activation instead of collisions, but is similar to CID in that dissociation is the result of slow thermal excitation.[28] In quadrupole ion trap mass spectrometers, IRMPD in comparison to CID offers the advantages of allowing trapping and detection of low mass product ions as well as consecutive activation and dissociation of primary product ions, both features which result in a larger array of fragment ions.[28, 29] Furthermore, since phosphate groups strongly absorb 10.6 μm photons, phosphorylated species are more readily dissociated compared to their non-phosphorylated counterparts; thus, selective

differentiation is possible. This unique IRMPD capability has been used to differentiate phosphorylated from unphosphorylated peptides as well as phosphate-containing cross-linked peptides from non-cross-linked species in complex mixtures.[30-33] IRMPD has recently been employed alongside CID in an FTICR mass spectrometer for lipid A structural analysis to increase fragment ion production,[14, 15] but has not been utilized to selectively differentiate the phosphorylation status of intact lipid A species or its product ions. UV photoexcitation allows faster and higher internal energy deposition compared to IRMPD for those molecules possessing appropriate UV chromophores.[34] Although applied successfully for characterization of peptides,[35, 36] nucleic acids,[37] and oligosaccharides,[38] UVPD has not been utilized for evaluation of lipid A structures and represents a promising opportunity due to the complexity of these molecules. a-EPD has been shown to yield rich diagnostic structural information for an array of biopolymer anions (e.g., peptides, proteins, and DNA).[39-41] This hybrid method uses UV irradiation (at ~260 nm in references 31-33) to produce charge-reduced radical anions that are subsequently isolated and subjected to collisional activation, yielding significantly different fragmentation behavior compared to CID of even electron molecular ions. Recently, we used high-energy, 193 nm ultraviolet photodissociation (UVPD) to promote fragmentation and electron photodetachment to characterize nucleic acids containing structural modifications; both 193 nm photodissociation alone as well as a-EPD yielded a more rich and impressive array of diagnostic product ions compared to CID.[37] Due to the success of these photon- and radical-directed dissociation techniques for other classes of biopolymers, we were motivated to apply these strategies to enhance the characterization of lipid A structures.

In this report, various lipid A species with significant structural diversity (see Supplemental Figure 1) were characterized using CID, IRMPD at 10.6 μm, UVPD at 193 nm, and a-EPD. The variation in the fragmentation patterns and complementary diagnostic pathways afforded by these methods make them a powerful tool box for the challenges posed by lipid A structures.

EXPERIMENTAL SECTION

Materials

Lipid A was isolated from *Helicobacter pylori* strain J99, *Campylobacter jejuni* strain 81-176, and *E. coli* MST10 using previously described methods.[42-44] The details of these materials can be found in the supplemental information. *E. coli* F583 lipid A and lipid IV_A were purchased from Sigma-Aldrich (St. Louis, MO) and Peptides International (Louisville, KY), respectively. All solvents were obtained from Fisher scientific (Fairlawn, NJ).

Mass spectrometry, Infrared Multiphoton Dissociation, and Ultraviolet Photodissociation

All mass spectrometric experiments were undertaken on a Thermo Fisher Scientific LTQ XL (San Jose, CA) using laser setups similar to that previously described.[33, 36] IRMPD and UVPD were performed using a 10.6 μm Synrad 50-W continuous wave CO_2 laser (model 48-5; Mukilteo, WA) and a 193 nm Coherent ExciStar XS excimer laser (Santa Clara, CA), respectively. Deprotonated lipid A anions were generated by electrospray ionization operated in the negative ion mode. Details of the experimental setup can be found in the supplemental information.

RESULTS AND DISCUSSION

Electrospray ionization of each lipid A yielded either both $[M - 2H]^{2-}$ and $[M - H]^-$ ions if two phosphorylation sites were present (such as for lipid IV_A and *E. coli* F583 lipid A) or only $[M - H]^-$ ions if only one phosphate was present (such as for *H. pylori* lipid A). In this

report, the $[M - H]^-$ ion was selected for comparisons between the various activation methods since CID of the $[M - 2H]^{2-}$ ions yielded significantly less fragmentation information compared to the singly charged ions (data not shown). It is of interest to note that the product ion distributions arising from UVPD at 193 nm were similar for both the 1- and 2- charge states. Finally, a-EPD experiments utilized the $[M - 2H]^{2-}$ precursor ion to create $[M - 2H]^{-\bullet}$ species (i.e. via UV photodetachment); and therefore, were only applicable to those lipid A species containing two phosphate groups.

To streamline the presentation of multiple complex MS/MS patterns and fragmentation pathways, the results are condensed into fragmentation schemes that indicate the cleavage sites (which are numbered) that produce particular types of fragment ions for each lipid A structure as well as lists of the *m/z* values of fragment ions that arise from those cleavage sites. These cleavage sites are assigned based on comparison of the MS/MS spectra of an array of lipid A structures. The majority of the dominant cleavage pathways observed for CID of the structures herein have been observed previously along with confirmation of genealogical relationships by MS^n.[6, 9, 11, 12, 15, 45] Depending on which lipid A is being characterized, it is possible to have degenerate fragmentation pathways that yield product ions with the same *m/z* values (e.g., it is not known from which fatty acid chain a particular alkyl group might be lost). However, for simplicity, only one representative cleavage site was marked for the schemes in Figures 2 through 4. Note that even ultra high mass accuracy measurements could not resolve the questions about cleavages of specific alkyl chains because the masses of the alkyl groups for some of different chains are identical. In the lists of *m/z* values to the right of each lipid structure in Figures 2 to 4, the ions are categorized according to the cleavages that result in their formation. For example, the *m/z* value of an ion that arises from three consecutive cleavages would be listed next to three cleavage numbers. The schemes concisely convey the dominant types of cleavages as well as showcasing the greater diversity of cleavages upon IRMPD, UVPD and a-EPD compared to CID. Key cleavages seen for UVPD and a-EPD that were not observed for CID or IRMPD are marked with a dashed red line instead of a dashed black line in Figures 2 to 4.

Dissociation of Lipid IV_A

Lipid IV_A is phosphorylated at the 4' and 1 positions of the glucosamines and contains four primary acyl chains (linked at the 2, 3, 2', and 3' sites). The CID mass spectrum of the singly charged lipid IV_A anion is shown in Figure 1a, and the corresponding fragmentation diagram, which matches *m/z* values from the MS/MS spectrum to cleavage sites along the structure, is illustrated in Figure 2a. The dominant product ions as seen in Figure 2a stemmed from neutral losses of phosphoric acid (cleavage (1)), and the loss of 3- and 3'-linked acyl chains (cleavages (2), (4), (6), and (7)). These pathways represented cleavages of specific C-O bonds that are labile upon collisional activation. The uninformative neutral loss of water was also a prevalent pathway.

The analogous IRMPD spectrum and fragmentation diagram of the same charge state are shown in Figures 1b and 2b, respectively. Although both CID and IRMPD are similar step-wise thermal heating processes,[28] there are striking absences of two product ions in the IRMPD spectrum (*m/z* 1159.67 and 1385.75) which in fact are products that retain both phosphate groups. As described in the Introduction, phosphate groups have very high photoabsorption cross-sections at 10.6 μm, thus promoting fast and efficient activation and photodissociation of phosphorylated species with rates that correlate with the number of phosphate groups.[30, 32] This enhanced IRMPD of phosphorylated species manifests itself as rapid annihilation of bis-phosphorylated product ions upon exposure to additional IR photons during the 30 ms irradiation period in the ion trap. Enhanced IR photodissociation of phosphorylated species has been reported previously[30] and allows selective differentiation of products ions that have various degrees of phosphorylation,[30, 32, 33] as also

evidenced in the present study. For example, CID produced bis-phosphorylated ions of *m/z* 1159.67 and 1385.67, and these ions were not observed in the corresponding IRMPD spectrum (Figure 1b) due to rapid photoabsorption and sequential dissociation (see red arrows showing the annihilation of these products). All other products had zero or one phosphate groups and thus remained as stable ions in the IRMPD mass spectrum. Although lipid IV_A has a fairly simple structure, the ability of IRMPD to selectively reveal the phosphorylation status of diagnostic products affords a useful tactic for screening product ions and aiding their structural assignment. The utility of this technique as applied to a more complex structure will be illustrated for *E. coli* F583 lipid A later in this report. A few low abundance product ions in the lower *m/z* range, including ions of *m/z* 332.25, 350.25, 368.25, and 448.25, were detected upon IRMPD that were not observed in the CID spectrum. These ions all arise from an inter-ring glucosamine cleavage (cleavage (9)) and the neutral loss of either the 3- or 3'-linked acyl chain in conjunction with additional neutral losses of water (18 Da) and/or a phospho moiety (80 Da). These additional product ions arise from sequential photodissociation of primary fragment ions and enhance the MS/MS fingerprint for lipid A structures.

In contrast to CID and IRMPD, 193 nm UV photodissociation and a-EPD yielded significantly different fragmentation patterns. The UVPD mass spectrum and resulting fragmentation map of lipid IV_A are shown in Figure 1c and Figure 2c, respectively. These figures illustrate that UVPD promotes C-C cleavages along the acyl chains and inter- and cross-ring glucosamine cleavages (i.e., cleavages (11), (13), and (15), and (9), (12), (17), and (18), respectively). Several products from C-O cleavages and losses of phosphoric acid (similar to those seen upon CID and IRMPD) were also observed. Interestingly, two product ions were observed from specific C-C cleavages adjacent to hydroxyl groups (cleavage sites (11) and (13)). We speculate that these unique cleavage sites are enhanced due to the partial carbonyl/oxide character of the alcohol group via sharing of the hydroxyl hydrogen through noncovalent, hydrogen-bonding interactions coupled with the fast, high energy deposition of UV photoirradiation that can access higher energy states. The prevalence of C-C cleavages next to carbonyl groups has been observed previously for peptide anions after 193 nm photodissociation,[46] as well as in this study (especially for *E. coli* F583 lipid A as illustrated in a subsequent section). Lastly, UVPD yielded abundant products from cleavages between the amine and carbonyl groups of either 2- or 2'-linked acyl chains (marked as cleavage (14) and corresponding to ions of *m/z* 1175.58 (only cleavage (14)), 1078.50 (both cleavages (1) and (14)), and 591.25 (cleavages (1), (7), and (14), Figure 2c). This unique preferential cleavage was confirmed by analyzing many different lipid A species by UVPD (data not shown), and proves useful for mapping modifications and confirming structural assignments of 2- or 2'-linked acyl chains because they don't generally cleave upon CID or IRMPD.

The fragmentation behavior and many of the resulting products observed for UVPD of the $[M - H]^-$ ion were also seen upon a-EPD of the $[M - 2H]^{-\bullet}$ ion (Figure 1d and Figure 2d). As mentioned previously, a-EPD entailed UV photoirradiation of the $[M - 2H]^{2-}$ precursor charge state to create charge-reduced radical species $[M - 2H]^{-\bullet}$ via loss of one electron, the latter which were then subsequently subjected to collisional activation. In the process of this radical-directed dissociation, hydrogen migration can occur within long-lived radical product ions (ones trapped and subjected to MS^3), and often the *m/z* values for the presumed same product ions differ by one Da (one hydrogen) when comparing the 193 nm UV photodissociation and a-EPD spectra. This occurrence has been observed previously in studies examining the dissociation of peptide radical species,[47-50] and is attributed to migration of hydrogen atoms and the radical electron sites within the intact precursors prior to dissociation or within the resulting fragment ions. This hydrogen migration phenomenon actually poses little problem for lipid A analysis because the majority of the predictable fragmentation sites differ in mass by significantly more than one or two Da, and the selected

precursors are typically singly charged (unlike peptide analysis in which several amino acids differ by 2 Da or less). In contrast to UVPD, a-EPD promoted an enhanced cross-ring cleavage at *m/z* 1261.75 (cleavage (19)), and enhanced cleavages next to carbonyls on the fatty acid chains (cleavages (6) and (20)). Decreased abundances and numbers of products due to loss of the phosphate moieties were also observed.

Dissociation of *E. coli* F583 lipid A

Each of the glucosamine groups of *E. coli* F583 lipid A is phosphorylated, and this lipid contains four primary acyl chains (linked at the 2, 3, 2', and 3' sites) as well as 2'- and 3'-linked secondary acyl chains. Due to the extra secondary acyl chains, this lipid A branching pattern is significantly more complex than that of lipid IV_A. The CID mass spectrum of the singly deprotonated *E. coli* F583 lipid A anion, $[M - H]^-$, is shown in Supplementary Figure 2a, and the corresponding fragmentation diagram is illustrated in Figure 3a. The dominant and most prevalent product ions again stemmed from neutral losses of phosphoric acid (cleavage (1)), and the loss of 3- and 3'-linked acyl chains (cleavages (2), (6), (7), and (8)). Another prominent pathway was the loss of 3'-linked secondary acyl chain (cleavage (11)). Less common (and lower in abundance) were cleavages of C-C bonds (i.e., one low abundance ion of *m/z* 1640.58 was identified which corresponded to the cleavage of the C-C bond adjacent to a carbonyl group of a secondary acyl chain, cleavage (10) in Figure 3a). A low abundance Y_1 inter-ring (C-O) glucosamine cleavage product was also detected at *m/z* 710.25 (cleavage (9)).

Since *E. coli* F583 lipid A yielded product ions retaining no, one or two phosphate groups upon CID, IRMPD could again be employed to differentiate these species as seen in Supplementary Figure 2b and Figure 3b. The selectivity noted in Supplementary Figure 2b is rather dramatic and aids product ion assignments when directly overlaid with CID spectra. For example, the red arrows extending from Supplementary Figure 2a to 2b show how the doubly phosphorylated product ions observed for CID are annihilated in the IRMPD mass spectrum. All other product ions seen in the IRMPD mass spectrum (Supplementary Figure 2b) are ones with a single or no phosphate group and are comparable to those observed in the CID spectrum (Supplementary Figure 2a). The IRMPD spectrum also reveals a few products of low *m/z* (*m/z* 332.17 and 448.17) associated with inter-ring glucosamine cleavages (i.e., Z_1 (14) and Y_1 (9) ions) that again expand the MS/MS fingerprint obtained from IRMPD.

The 193 UV photodissociation spectrum of the same singly charged lipid A (*E. coli* F583) and the associated fragmentation map are presented in Supplementary Figure 2c and Figure 3c, respectively. UVPD again yielded different fragmentation trends compared to CID and IRMPD, but generally similar to that described above for lipid IV_A including favored products from C-C cleavages, glucosamine cleavages, and cleavages between the amine and carbonyl groups on the 2- and 2'-linked primary acyl chains. One general type of C-C bond cleavage which was particularly prevalent and yielded product ions with high abundances occurred adjacent to the carbonyl groups on the fatty acid chains (denoted as cleavages (10), (13), and (17) in Figure 3c). The a-EPD spectrum and fragmentation map for *E. coli* are shown in Supplementary Figure 2d and Figure 3d. Similar to 193 nm UV photodissociation, a-EPD also yielded many high abundance products via C-C cleavages adjacent to carbonyl groups on the fatty acid chains, but the site selectivity was slightly different (comparing cleavages (21) and (23) Figure 3d with (10), (13), and (17) in Figure 3c). Two extra glucosamine cleavages were also seen for a-EPD in Figure 3d (cleavages (20) and (22)) that were not observed upon UVPD (Figure 3c).

Dissociation of *H. pylori* wild type Lipid A

Unlike the other lipids, *H. pylori* lipid A has no 3'-linked acyl chain and is modified with one phosphorylethanolamine moiety. The MS/MS and fragmentation behavior diagram for CID of *H. pylori* lipid A are shown in Supplementary Figure 3a and Figure 4a, respectively. Like the other lipid A species in this study, C-O cleavages along the fatty acid chains was the most efficient fragmentation pathways upon CID. Interestingly, several products originated from C-C cleavage adjacent to carbonyl groups (cleavages (5) and (7) as denoted in Figure 4a); a trend more commonly observed upon a-EPD and UVPD. Since these products were not observed upon CID of the other structurally similar lipid A species, we speculate that the phosphorylethanolamine promotes this unusual fragmentation behavior.

UVPD again resulted in several products from inter- and cross-ring glucosamine cleavages with high abundances as well as fatty acid cleavages at C-C bonds as illustrated in Supplemental Figure 3b and Figure 4b. What is notably different for the UVPD spectrum of this lipid A species is the presence of the highly abundant product of *m/z* 1504.17 in Supplemental Figure 3b (denoted as cleavage (20) in Figure 4b). This ion corresponded to loss of 43 Da from the precursor, consistent with the elimination of ethanolamine from the phosphorylethanolamine modification. Several other products of lower *m/z* also exhibited the loss of ethanolamine (*m/z* 1472.75, 1445.08, 1428.17, 1221.83, and 1293.00), albeit with significantly lower abundances. To determine whether the 43 Da neutral loss was uniquely characteristic of phosphorylethanolamine-modified lipids, two other phosphorylethanolamine modified lipid A species from *C. jejuni* and *E. coli* (see structures in Supplementary Figure 4) were also investigated by UVPD. Both lipids generated the same 43 Da neutral loss from the precursor. This particular ion was again the dominant product in the spectra (data not shown) and was never observed upon CID nor upon UVPD of any other species lacking the phosphorylethanolamine group. Such a highly preferential cleavage by UVPD may allow selective identification of phosphorylethanolamine-modified lipid A species by rapid, MS-based screening methods. This example again illustrates the benefits of using multiple MS^n methods that promote different types and modes of energy deposition as analytical tools for the characterization of lipid A structures.

CONCLUSIONS

Low energy CID, IRMPD, UVPD, and a-EPD methods all yield different cleavage selectivities and thus can be utilized in a complementary fashion for the most complete characterization of lipid A structures and its many modifications. While CID alone has proven to be beneficial, vast amounts of MS^n data are often required to increase the success of species-specific characterization. Employing methods such as IRMPD, 193 nm UVPD, and a-EPD that generate different fragmentation selectivities increase the chances of validating structure assignments and successfully pinpointing subtle modifications. For example, UVPD promotes cross-ring cleavages, carbon-carbon cleavages along the acyl chains, especially ones adjacent to carbonyl and hydroxyl groups, in addition to cleavages of the amide bond linkages. IRMPD allows differentiation of the phosphorylation status of specific diagnostic product ions. Lastly, development of automated computational methods, such as those developed for CID patterns of lipids,[51] that can exploit the unique fragmentation behavior of all these complementary dissociation methods would facilitate the most extensive, efficient, and sensitive lipid A structural assignments.

Supplementary Material

Refer to Web version on PubMed Central for supplementary material.

Acknowledgments

J.S.B. acknowledges funding from the NSF (CHE-1012622), and the Welch Foundation (F-1155). J.A.M. acknowledges the ACS division of Analytical Chemistry and The Society for Analytical Chemists of Pittsburgh for support. M.S.T. acknowledges funding from the NIH (Grants AI064184 and AI76322).

References

1. Raetz CR, Reynolds CM, Trent MS, Bishop RE. Annu Rev Biochem. 2007; 76:295–329. [PubMed: 17362200]
2. Trent MS, Stead CM, Tran AX, Hankins JV. J Endotoxin Res. 2006; 12:205–223. [PubMed: 16953973]
3. Banoub JH, El Aneed A, Cohen AM, Joly N. Mass Spectrom Rev. 2010; 29:606–650. [PubMed: 20589944]
4. Chan S, Reinhold VN. Anal Biochem. 1994; 218:63–73. [PubMed: 8053569]
5. Boue SM, Cole RB. J Mass Spectrom. 2000; 35:361–368. [PubMed: 10767765]
6. Kussak A, Weintraub A. Anal Biochem. 2002; 307:131–137. [PubMed: 12137789]
7. El-Aneed A, Banoub J. Rapid Commun Mass Spectrom. 2005; 19:1683–1695. [PubMed: 15912470]
8. Murphy RC, Raetz CRH, Reynolds CM, Barkley RM. Prostaglandins Other Lipid Mediators. 2005; 77:131–140. [PubMed: 16099398]
9. Lee C-S, Kim Y-G, Joo H-S, Kim B-G. J Mass Spectrom. 2004; 39:514–525. [PubMed: 15170747]
10. Wang Z, Li J, Altman E. Carbohydr Res. 2006; 341:2816–2825. [PubMed: 17049500]
11. Mikhail I, Yildirim HH, Lindahl ECH, Schweda EKH. Anal Biochem. 2005; 340:303–316. [PubMed: 15840504]
12. Madalinski G, Fournier F, Wind F-L, Afonso C, Tabet J-C. Int J Mass Spectrom. 2006; 249/250:77–92.
13. Silipo A, De Castro C, Lanzetta R, Molinaro A, Parrilli M, Vago G, Sturiale L, Messina A, Garozzo D. J Mass Spectrom. 2008; 43:478–484. [PubMed: 17975853]
14. Jones JW, Shaffer SA, Ernst RK, Goodlett DR, Turecek F. Proc Natl Acad Sci U S A. 2008; 105:12742–12747. [PubMed: 18753624]
15. Jones JW, Cohen IE, Turecek F, Goodlett DR, Ernst RK. J Am Soc Mass Spectrom. 2010; 21:785–799. [PubMed: 20185334]
16. Shaffer SA, Harvey MD, Goodlett DR, Ernst RK. J Am Soc Mass Spectrom. 2007; 18:1080–1092. [PubMed: 17446084]
17. Kaltashov IA, Doroshenko V, Cotter RJ, Takayama K, Qureshi N. Anal Chem. 1997; 69:2317–2322. [PubMed: 9212704]
18. Johnson RS, Her GR, Grabarek J, Hawiger J, Reinhold VN. J Biol Chem. 1990; 265:8108–8116. [PubMed: 2335519]
19. Phillips NJ, Apicella MA, Griffiss JM, Gibson BW. Biochemistry. 1992; 31:4515–4526. [PubMed: 1581306]
20. Spengler B, Dolce JW, Cotter RJ. Anal Chem. 1990; 62:1731–1737.
21. Spengler B, Kirsch D, Kaufmann R, Lemoine J. Org Mass Spectrom. 1994; 29:782–787.
22. Gage DA, Rathke E, Costello CE, Jones MZ. Glycoconjugate J. 1992; 9:126–131.
23. Solouki T, Reinhold BB, Costello CE, O'Malley M, Guan S, Marshall AG. Anal Chem. 1998; 70:857–864. [PubMed: 9511464]
24. Coates ML, Wilkins CL. Biomed Mass Spectrom. 1985; 12:424–428. [PubMed: 2931133]
25. Coates ML, Wilkins CL. Anal Chem. 1987; 59:197–200. [PubMed: 3826629]
26. Takayama K, Qureshi N, Hyver K, Honovich J, Cotter RJ, Mascagni P, Schneider H. J Biol Chem. 1986; 261:10624–10631. [PubMed: 3090037]
27. Zhou Z, Ogden S, Leary JA. J Org Chem. 1990; 55:5444–5446.
28. Brodbelt JS, Wilson JJ. Mass Spectrom Rev. 2009; 28:390–424. [PubMed: 19294735]
29. Madsen JA, Brodbelt JS. J Am Soc Mass Spectrom. 2009; 20:349–358. [PubMed: 19036605]

30. Flora JW, Muddiman DC. Anal Chem. 2001; 73:3305–3311. [PubMed: 11476230]
31. Flora JW, Muddiman DC. J Am Chem Soc. 2002; 124:6546–6547. [PubMed: 12047170]
32. Crowe MC, Brodbelt JS. Anal Chem. 2005; 77:5726–5734. [PubMed: 16131088]
33. Gardner MW, Vasicek LA, Shabbir S, Anslyn EV, Brodbelt JS. Anal Chem. 2008; 80:4807–4819. [PubMed: 18517224]
34. Reilly JP. Mass Spectrom Rev. 2009; 28:425–447. [PubMed: 19241462]
35. Kim T-Y, Thompson MS, Reilly JP. Rapid Commun Mass Spectrom. 2005; 19:1657–1665. [PubMed: 15915476]
36. Madsen JA, Boutz DR, Brodbelt JS. J Proteome Res. 2010; 9:4205–4214. [PubMed: 20578723]
37. Smith SI, Brodbelt JS. Anal Chem. 2010; 82:7218–7226. [PubMed: 20681614]
38. Devakumar A, Thompson MS, Reilly JP. Rapid Commun Mass Spectrom. 2005; 19:2313–2320. [PubMed: 16034827]
39. Gabelica V, Tabarin T, Antoine R, Rosu F, Compagnon I, Broyer M, De Pauw E, Dugourd P. Anal Chem. 2006; 78:6564–6572. [PubMed: 16970335]
40. Antoine R, Joly L, Tabarin T, Broyer M, Dugourd P, Lemoine J. Rapid Commun Mass Spectrom. 2007; 21:265–268. [PubMed: 17167813]
41. Larraillet V, Antoine R, Dugourd P, Lemoine J. Anal Chem. 2009; 81:8410–8416. [PubMed: 19775153]
42. Tran AX, Whittimore JD, Wyrick PB, McGrath SC, Cotter RJ, Trent MS. J Bacteriol. 2006; 188:4531–4541. [PubMed: 16740959]
43. Cullen TW, Trent MS. Proc Natl Acad Sci U S A. 2010; 107:5160–5165. [PubMed: 20194750]
44. Tran AX, Karbarz MJ, Wang X, Raetz CR, McGrath SC, Cotter RJ, Trent MS. J Biol Chem. 2004; 279:55780–55791. [PubMed: 15489235]
45. Gaucher SP, Cancilla MT, Phillips NJ, Gibson BW, Leary JA. Biochemistry. 2000; 39:12406–12414. [PubMed: 11015221]
46. Madsen JA, Kaoud TS, Dalby KN, Brodbelt JS. Proteomics. 2011 in press.
47. Swaney DL, McAlister GC, Wirtala M, Schwartz JC, Syka JEP, Coon JJ. Anal Chem. 2007; 79:477–485. [PubMed: 17222010]
48. Madsen JA, Brodbelt JS. Anal Chem. 2009; 81:3645–3653. [PubMed: 19326898]
49. O'Connor PB, Lin C, Cournoyer JJ, Pittman JL, Belyayev M, Budnik BA. J Am Soc Mass Spectrom. 2006; 17:576–585. [PubMed: 16503151]
50. Ledvina AR, McAlister GC, Gardner MW, Smith SI, Madsen JA, Schwartz JC, Stafford GC Jr, Syka JEP, Brodbelt JS, Coon JJ. Angew Chem Int Ed. 2009; 48:8526–8528.
51. Ting YS, Shaffer SA, Jones JW, Ng WV, Ernst RK, Goodlett DR. J Am Soc Mass Spectrom. 2011; 22:856–866. [PubMed: 21472520]

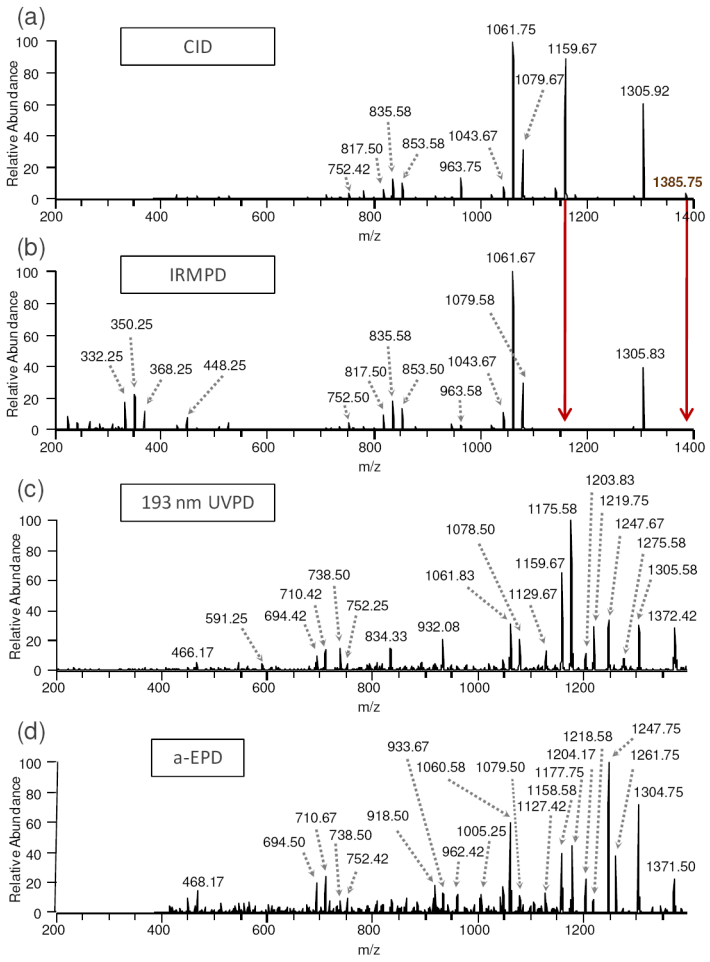

Figure 1.

MS/MS spectra from the dissociation of lipid IV_A by (a) CID, 1-, (b) IRMPD, 1-, (c) 193 nm UVPD, 1-, and (d) a-EPD, 1-•. Red arrows highlight the product ions that undergo sequential IRMPD. The 1- precursor was *m/z* 1403.8 and the 1-• precursor (for a-EPD) was *m/z* 1402.8.

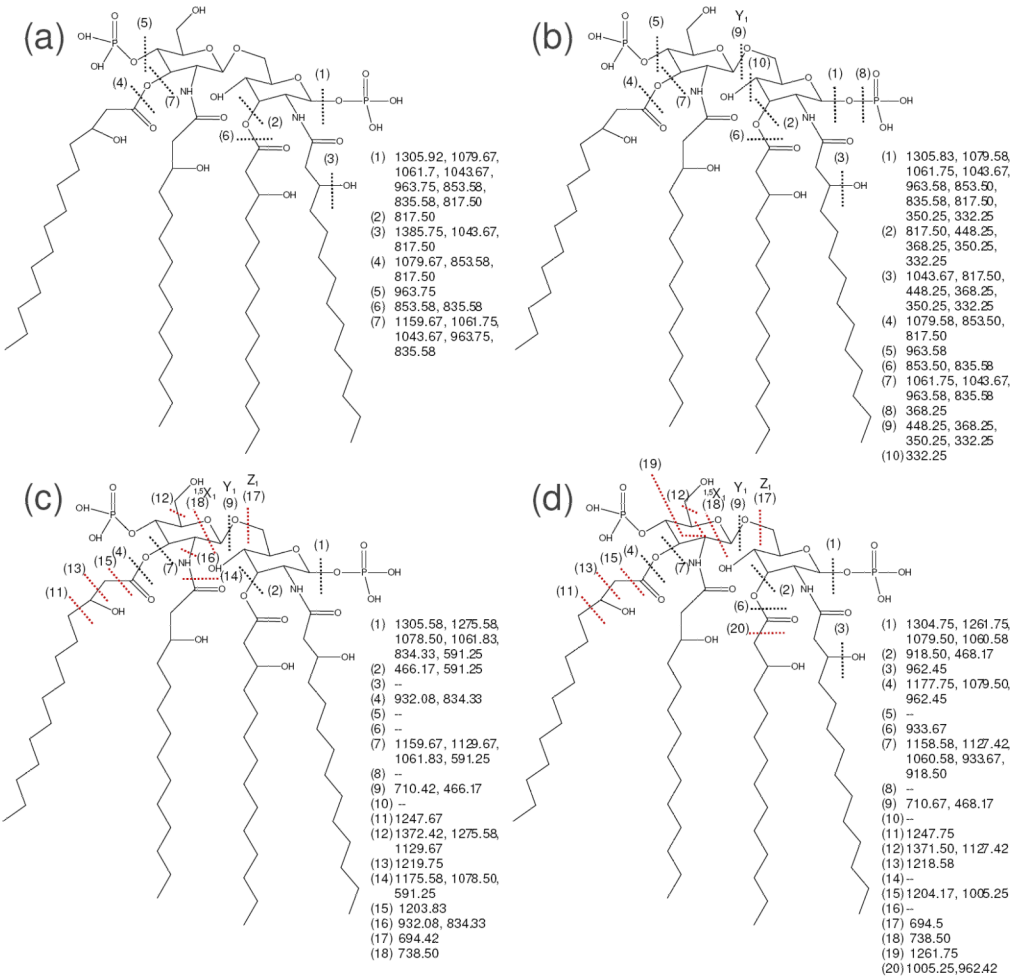

Figure 2.

Fragmentation behavior of lipid IV_A by (a) CID, 1-, (b) IRMPD, 1-, (c) 193 nm UVPD, 1-, and (d) a-EPD, 1-•. Dashed lines represent cleavage sites, and are matched with the *m/z* values to the right of the structure, which were taken from the representative mass spectrum (Figure 1). Key cleavages seen for UVPD and a-EPD that were not observed for CID or IRMPD are marked with red lines.

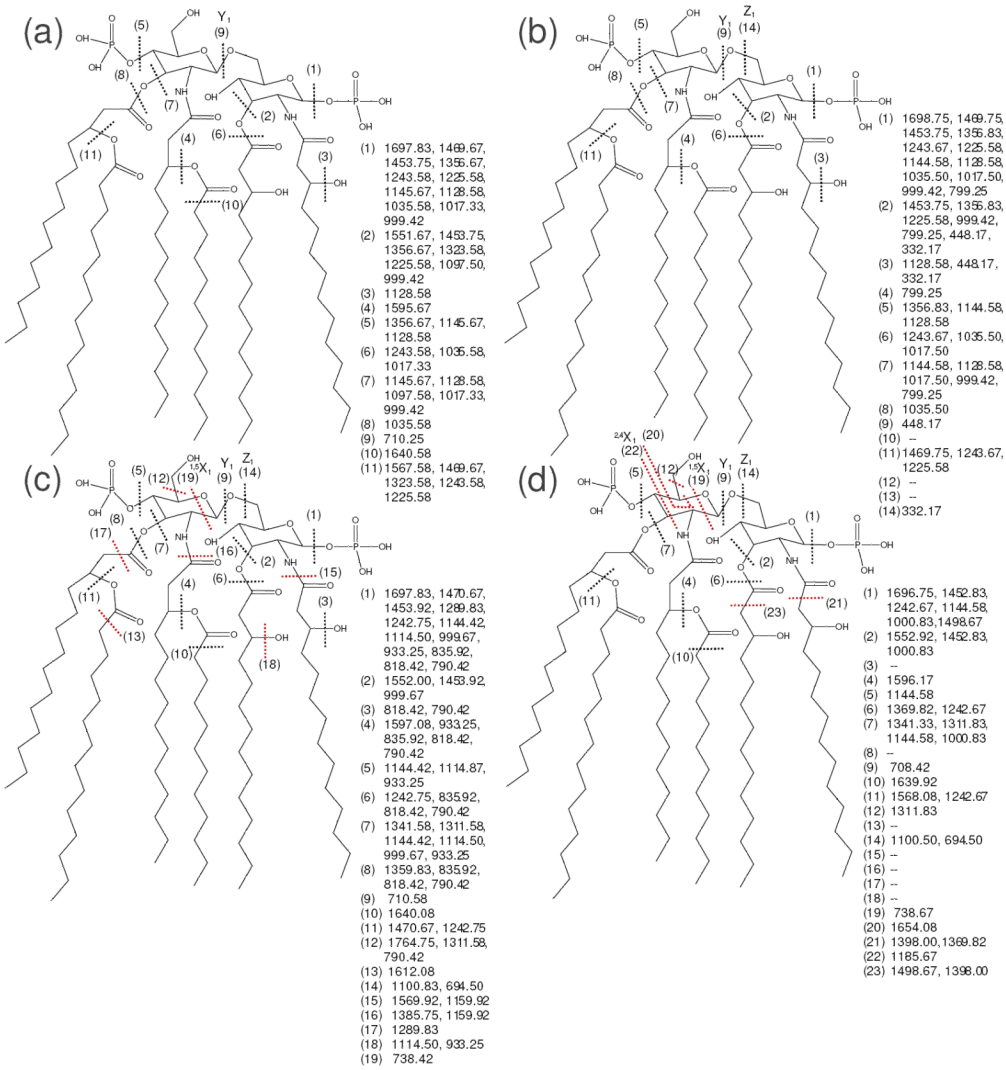

Figure 3.

Fragmentation behavior of *E. coli* F583 lipid A by (a) CID, 1-, (b) IRMPD, 1-, (c) 193 nm UVPD, 1-, and (d) a-EPD, 1-•. Dashed lines represent cleavage sites, and are matched with the *m/z* values to the right of the structure, which were taken from the representative mass spectrum (Supplemental Figure 1). Key cleavages seen for UVPD and a-EPD that were not observed for CID or IRMPD are marked with red lines.

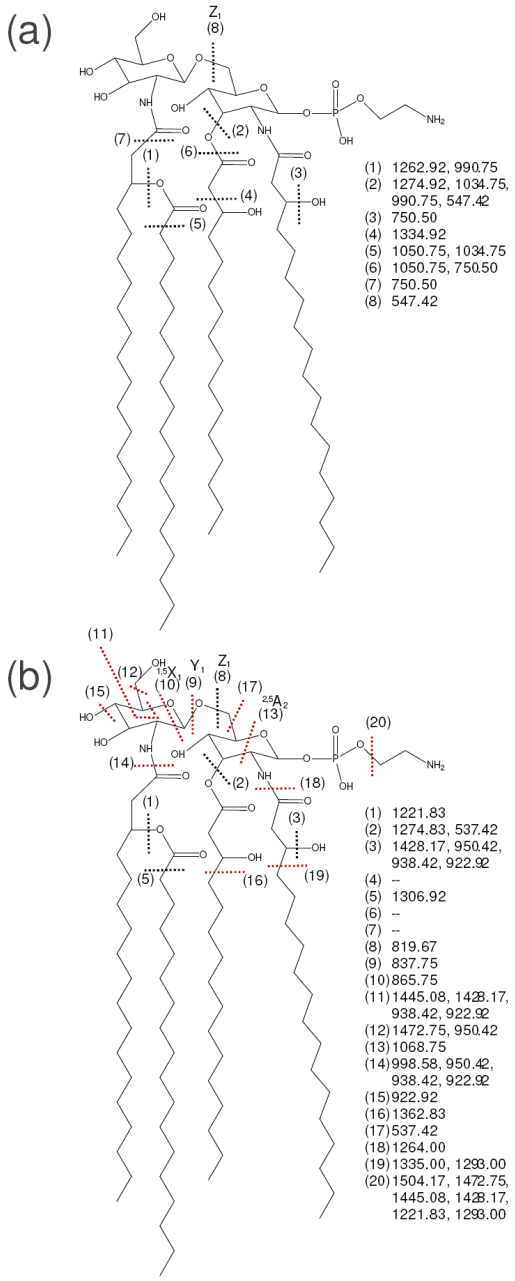

Figure 4.

Fragmentation behavior of *H. pylori* lipid A (MW 1548.2) by (a) CID, 1-, and (b) 193 nm UVPD, 1-. Dashed lines represent cleavage sites, and are matched with the *m/z* values to the right of the structure, which were taken from the representative mass spectrum (Supplemental Figure 2). Key cleavages seen for UVPD and a-EPD that were not observed for CID or IRMPD are marked with red lines.